

Performance Analysis of Hybrid HVDC Transmission Systems for Connecting Offshore Wind Farm to Onshore Grid

Ann Maria Isaac¹, K Rathi²MTech Student, Dept of Electrical and Electronics, Government Engineering College Thrissur, Kerala, India¹Associate Professor, Dept of Electrical and Electronics, Government Engineering College Thrissur, Kerala, India²

ABSTRACT: This paper presents the performance analysis of DFIG based off shore wind farm feeding to large power system through a hybrid HVDC link. The hybrid HVDC link consists of a line commutated converter based inverter and voltage source converter based rectifier. The active and reactive power of off shore station is controlled using voltage source converter based rectifier controller and the dc line voltage is maintained constant at line commutated inverter station control. The hybrid HVDC transmission system gives many advantages over conventional HVDC transmission systems. Time domain method based on non linear model simulation using MATLAB is performed to analyze the performance of the studied system

KEYWORDS: DFIG wind farm; hybrid HVDC.

I. INTRODUCTION

Wind energy system has gained vast populations in the past decade as one of the renewable energy resources due to the possibility of depletion of conventional energy resources and their high cost. As the capacity of land based wind farms grows, shortage of available land resources and environmental concerns has become increasingly critical. Since wind energy is abundantly available and space is less restricted at sea, off shore wind farm have drawn broad attention in recent years. One of the major challenges of off shore wind farm is how to increase the transmission distance between off shore power generation and on shore distribution grid. HVDC is a viable solution for this.

There are two different converters used for HVDC transmission technologies, i.e. VSC using controllable switches like insulated-gate bipolar transistors (IGBTs) [1], and CSC or line-commutated converter (LCC) using controllable switches such as thyristors [2]. The LCCs have been widely used for HVDC links for several ten years since they can be used for very high power level and have less power losses when comparing with VSC-based HVDC links. However, when the AC system connected to the LCC is weak, this brings inherent difficulty in continuing reliable commutation. The VSC can control active and reactive power independently and quickly regardless of the AC system conditions while no communication is required between two VSC stations.

Hybrid transmission system for connecting two AC systems is aimed at combining the advantages of both HVDC technologies and compensating the above mentioned drawbacks. The basic structure of a hybrid HVDC link with a conventional HVDC converter at the sending side and a VSC at the receiving side was proposed in [3]. A solution for integrating OWFs feeding into an onshore main grid through a hybrid HVDC link was described in [4] while this hybrid HVDC proposed an LCC and a VSC for the rectifier and the inverter, respectively. A new hybrid HVDC interconnector comprised a thyristor-based HVDC converter with series capacitors and a VSC-based static synchronous compensator (STATCOM) with island loads fed presented in [5].

The hybrid HVDC option discussed in this work has line commutated inverter and voltage source converter based rectifier. Because the hybrid HVDC link uses different converters, this new configuration can offer several advantages over conventional HVDC links. In other words, the VSC can offer more flexible power control of wind farms. VSC at off shore wind platform eliminated the need for STATCOM which reduces the off shore platform size. LCC can be used to maintain a constant dc voltage through the dc link. In spite of the above mentioned advantages, the hybrid HVDC system cannot reverse the power flow easily. However, only one power flow direction is required for offshore power generation.

This paper is organised as follows. Firstly the configuration of the studied system is explained including the design of DFIG wind farm. Next the hybrid HVDC transmission system with the control strategies is presented. Finally the performance of the system is analysed using simulation of the system in MATLAB and the results are presented.

II. CONFIGURATION OF THE STUDIED SYSTEM

Fig. 1 shows the configuration of the studied system consisting of a DFIG-based off shore wind farm (OWF) connected to the point of common coupling (PCC) through a hybrid HVDC link. The equivalent aggregated 9 MW DFIG driven by an equivalent aggregated variable- speed wind turbine (VSWT) through an equivalent aggregated gearbox (GB) is obtained by aggregating four 1.5-MW DFIGs. The output terminal of equivalent aggregated wind generator is connected to local load through a step-up transformer (0.575/25 kV) and undersea cable. The VSC connected to DC bus regulates the active and reactive power using a dq-axis reference frame controller while the onshore LCC connected to the PCC to maintain the DC voltage using a PI controller.

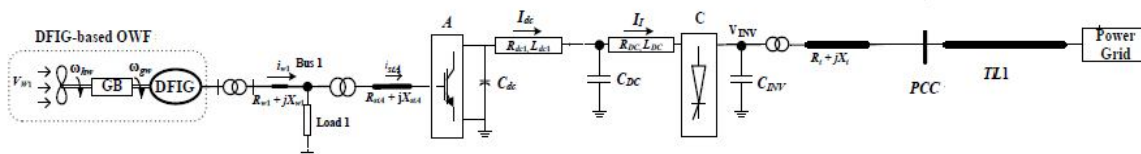


Fig 1: Configuration of hybrid HVDC for off shore wind farm feeding into power system

The mathematical models for the subsystems shown in Fig.1 are described as below. The equations in the following subsections are expressed in per unit (pu) except that the time variable t and the base angular frequency are in s and rad/s , respectively.

A. Variable-Speed Wind Turbine Model

The captured mechanical power by a VSWT from wind is given by

$$P_{mw} = \frac{1}{2} \rho_w \cdot A_w \cdot V_w^3 \cdot C_{pw}(\lambda_w, \beta_w) \quad (1)$$

where ρ_w is the air density (kg/m^3), A_w is the blade impact area (m^2), V_w is the wind speed (m/s), and C_{pw} is the dimensionless power coefficient of the VSWT which is a function of λ_w and β_w , λ_w is the tip speed ratio, β_w is blade pitch angle (degrees). The power coefficient of the VSWT C_{pw} is given by

$$C_{pw}(\lambda_w, \beta_w) = c_1 \left(\frac{c_2}{\psi_{kw}} - c_3 \beta_w - c_4 \beta_w^{c_5} - c_6 \right) \exp \left(-\frac{c_7}{\psi_{kw}} \right) \quad (2)$$

In which

$$\frac{1}{\psi_{kw}} = \frac{1}{\lambda_w + c_8 \beta_w} - \frac{c_9}{\beta_w^3 + 1} \quad (3)$$

$c_1 - c_9$ are the constant coefficients for power coefficient C_{pw} of the studied VSWT

B. DFIG Model

The stator windings of a wind DFIG are directly connected to the low-voltage side of the 0.575/25-kV step-up transformer while its rotor windings are connected through a rotor-side converter (RSC), a DC-link and a grid-side converter (GSC) to low voltage side of transformer.

For normal operation of a wind DFIG, the output AC-side voltages of the RSC and the GSC can be effectively controlled to achieve the required purposes. The pu dq-axis currents of the RSC are required to follow the varying reference points by maintaining the output active power and the stator-winding voltage at the setting values. The pu dq-axis currents of the GSC have to track the reference points by maintaining the DC link voltage at the setting value and keeping the output of the GSC at unity power factor

The control signals at grid side converter are given by the following equations

$$v_d = w_{gs}L_g i_{qg} + e_d + \Delta v_d$$

$$v_q = -w_{gs}L_g i_{dg} + e_q + \Delta v_q \tag{4}$$

Where $\tag{5}$

$$\Delta v_d = k_p(i_{dg}^* - i_{dg}) + k_i \int (i_{dg}^* - i_{dg}) dt \tag{6}$$

$$\Delta v_q = k_p(i_{qg}^* - i_{qg}) + k_i \int (i_{qg}^* - i_{qg}) dt \tag{7}$$

$$i_{dg}^* = k_p(v_{dc}^* - v_{dc}) + k_i \int (v_{dc}^* - v_{dc}) dt \tag{8}$$

And i_{qg}^* is zero.

Where v_d and v_q are the d axis and q axis control voltages, w_{gs} is the angular velocity of stator flux, L_g is the ac side inductance of rectifier, e_d and e_q are input voltages expressed in dq reference frame k_p and k_i are gains i_{qg}^* and i_{dg}^* are the reference values i_{qg} and i_{dg} are the measured value of stator current v_{dc}^* is the reference value of dc link voltage and v_{dc} is the measured dc link voltage.

The control equations for rotor side converter are given by equations (9- 12)

$$v_d = \Delta v_{dr} + i_{dr}R_r - \omega(L_{lr} + L_m)i_{qr} - \omega L_m i_{qs} \tag{9}$$

$$v_q = \Delta v_{qr} + i_{qr}R_r + \omega(L_{lr} + L_m)i_{dr} + \omega L_m i_{ds} \tag{10}$$

$$\Delta v_{dr} = K_p(i_{dr}^* - i_{dr}) + K_i \int (i_{dr}^* - i_{dr}) dt \tag{11}$$

$$\Delta v_{qr} = K_p(i_{qr}^* - i_{qr}) + K_i \int (i_{qr}^* - i_{qr}) dt \tag{12}$$

Where i_{dr} and i_{qr} are the measured rotor side currents i_{dr}^* and i_{qr}^* are the reference currents R_r is the rotor resistance L_{lr} is the leakage inductance and L_m is the magnetizing inductance K_p and K_i are the gains.

C. Hybrid HVDC Link Model

The hybrid HVDC link consists of 2-level VSC at sending end side connected to twelve pulse bridge LCC at receiving end side through a long distance transmission line. Turned filters and reactive compensation are considered at LCC. V_s in the equivalent scheme of hybrid HVDC represents the generator bus voltage of DFIG wind farm.

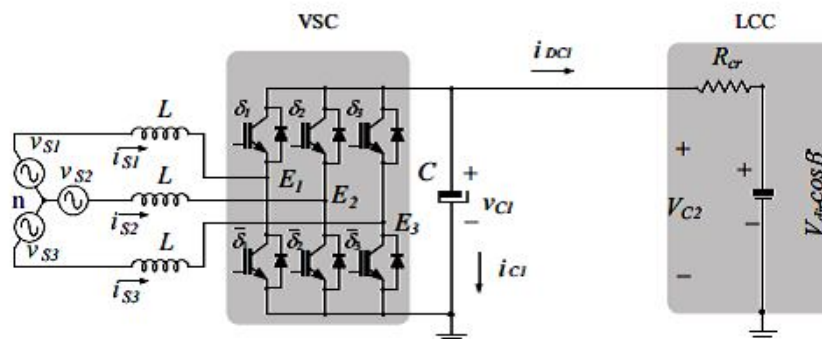


Fig.2. Equivalent scheme of hybrid HVDC

The dynamics of VSC can be represented by following model

$$v_S(t) = L \frac{d}{dt} i_S(t) + v_{C1}(t)(2I\delta(t) - I) \quad (13)$$

$$C \frac{d}{dt} v_{C1}(t) = \delta(t)^T i_S(t) - i_{DC1}(t) \quad (14)$$

v_S represents the wind farm phase voltages($[v_{S1}, v_{S2}, v_{S3}]^T$)
 i_S represents the phase currents of the wind farm($[i_{S1}, i_{S2}, i_{S3}]^T$)
 δ vector of switch positions

i_{DC1} is the dc current

v_{C1} is the dc voltage

L is the equivalent inductance of the VSC transformer

C is the capacitance of the dc filter

The VSC model in dq reference frame can be represented as

$$L \frac{d}{dt} i_{sdq} = v_{sdq} - v_{dq} - \omega L J i_{sdq} \quad (15)$$

$$C v_{C1} \frac{d}{dt} v_{C1} = v_{dq}^T i_{sdq} - v_{C1} i_{DC1} \quad (16)$$

Where $i_{sdq} = [i_{sd} \ i_{sq}]^T$, $v_{sdq} = [v_{sd} \ v_{sq}]^T$, $v_{dq} = [v_d \ v_q]^T$ represent the ac current, ac voltage and duty vector in dq coordinates, ω is the angular frequency of the reference phase voltage and

$J = \begin{bmatrix} 0 & -1 \\ 1 & 0 \end{bmatrix}$ is the anti symmetric matrix.

The dynamic of LCC can be expressed by the following model

$$v_{C2} = v_{dir} \cos \beta - i_{DC} R_{ci} \quad (17)$$

$$v_{dir} = \frac{3\sqrt{2}}{\pi} v_{LL} \quad (18)$$

$$R_{ci} = \frac{3}{\pi} \omega_2 L_c \quad (19)$$

where v_{C2} is the DC voltage in the DC link, β is the ignition advance angle, i_{DC} is the DC current in the DC link, v_{LL} represents the line-to-line voltage in the AC side, L_c is the inductance and ω_2 is the angular frequency in the AC side of the LCC.

D. Control Design

The control objective of VSC is to regulate active and reactive power to their references. Vector control in dq reference frame is used. The d axis is set in phase with V_S hence the d component is equal to V_S and q component is equal to 0.

Therefore active and reactive power are given by

$$P = \frac{3}{2} (v_{sd} \cdot i_{sd}) \quad (20)$$

$$Q = \frac{3}{2} (-v_{sd} \cdot i_{sq}) \quad (21)$$

Notice that if we set the d-axis as we described above the active power P is decoupled from reactive power Q , therefore if we consider constant v_{sd} , the active power P is related with i_{sd} and reactive power Q is related with i_{sq} , under this assumptions the control strategy is regulated the i_{sd} and i_{sq} toward its references i_{sd}^* and i_{sq}^* which will be constructed as follows:

$$i_{sd}^* = - \left(k_{p1} + \frac{k_{i1}}{s} \right) (p - p^*) \quad (22)$$

$$i_{sq}^* = - \left(k_{p1} + \frac{k_{i1}}{s} \right) (q - q^*) \quad (23)$$

The control voltages to VSC is given by

$$u_{cq} = \left(k_p + \frac{k_i}{s} \right) (i_{sq} - i_{sq}^*) - \omega L i_{sd} + u_{tq} \quad (24)$$

$$u_{cd} = \left(k_p + \frac{k_i}{s} \right) (i_{sd} - i_{sd}^*) + \omega L i_{sq} + u_{td} \quad (25)$$

Where u_t is the ac voltage input at the rectifier.

The control system of VSC based on a fast inner current control loop and an outer control loop. The outer loop consists

of active power controller and reactive power controller. The reference active current is obtained from active power controller and reference reactive power is derived from reactive power controller. The ac currents are controlled in inner current loop to obtain the modulating signal voltage for PWM generator. LCC controls the dc link voltage constant with the help of a PI controller

The control objective of LCC consists of designing a controller to regulate the DC voltage v_{C2} toward its reference v_d . The control objective can be interpreted as design γ_I , the extinction angle so that $V_{C2.ref} - V_d$ goes to zero.

$$T_Y \frac{d}{dt} (\Delta\gamma_I) = K_Y (V_{C2.ref} - V_d) - \Delta\gamma_I \tag{26}$$

The proposed control block diagrams for the VSCs and LCC of the hybrid HVDC system are shown in Figures.3 and 4 and 5 respectively.

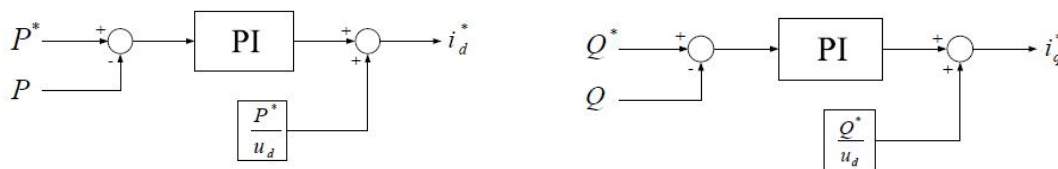


Fig.3.(a) block diagram of active power controller (b) Block diagram of reactive power controller

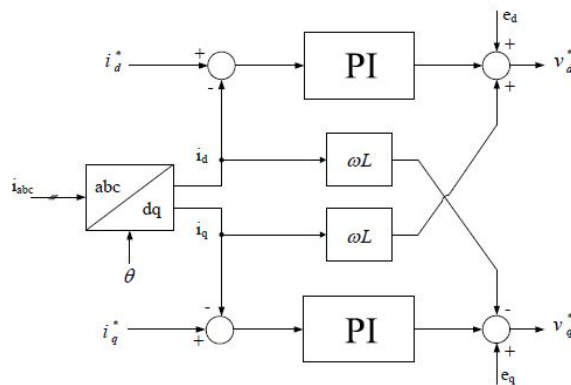


Fig.4. Block diagram of inner current loop controller

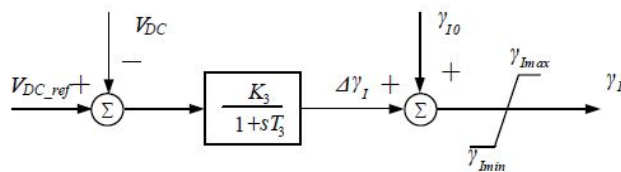


Fig.5. Block diagram of LCC controller

III. TIME DOMAIN SIMULATIONS

This section uses the non linear system model developed in previous section to demonstrate the effectiveness of the proposed control scheme of the hybrid HVDC system subject to different disturbances. Simulation results are performed using MATLAB/SIMULINK..

A. Variable Wind Speed

The performance of the system during variable wind speed are shown in figures 5 and 6. The wind speed is varying from 8m/s to 20 m/s during time 3s to 5s. The power generated by wind farm varies according to the wind speed. But the transmitted power is maintained at 1 pu. The reactive power at onshore side is regulated at 0 pu.

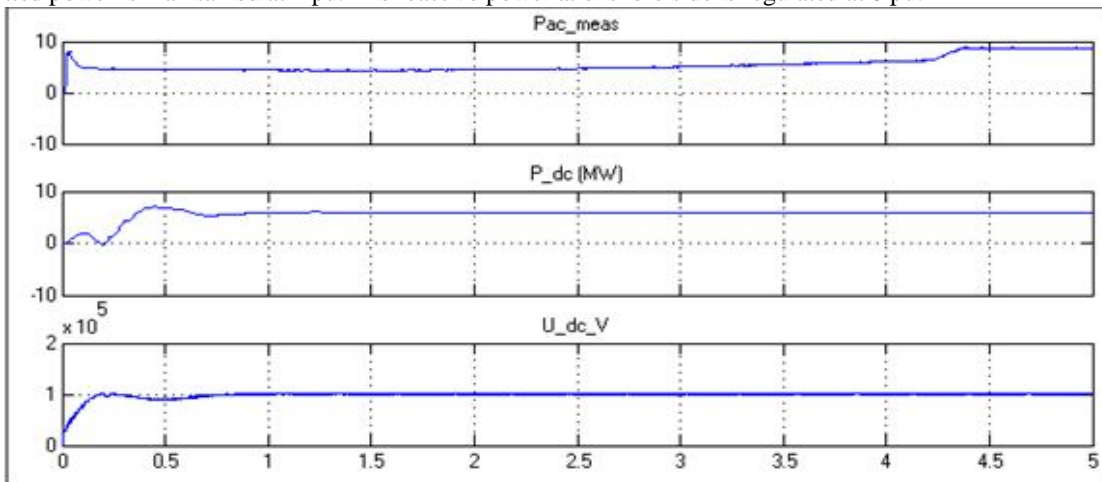


Fig.5.(a) generated power by DFIG (b) transmitted power (c) dc line voltage

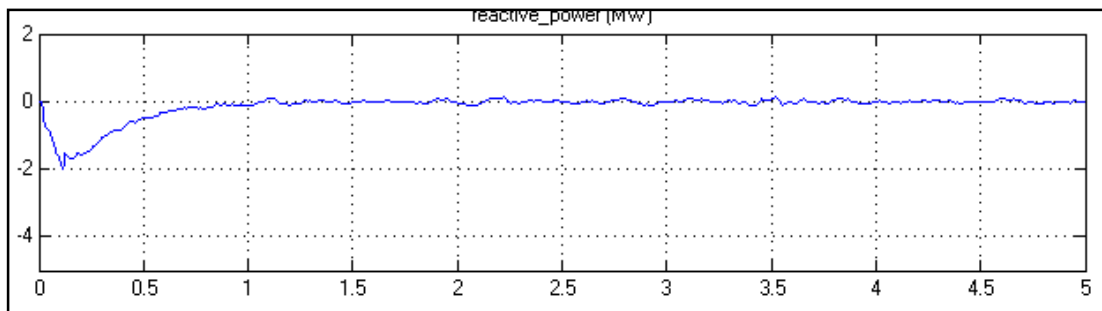


Fig.6.Reactive power at off shore

B. Fault at Infinite Grid

A three phase to ground fault occurs at the grid side at 4s and cleared at 4.1 s. The system recovered from fault with fairly good response time of 0.2s. Results of system response during grid fault is shown in figure 7.

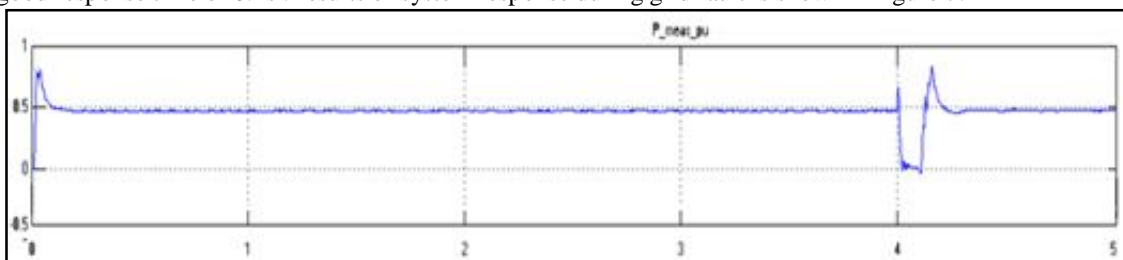


Fig. 7. (a) Active power transmitted

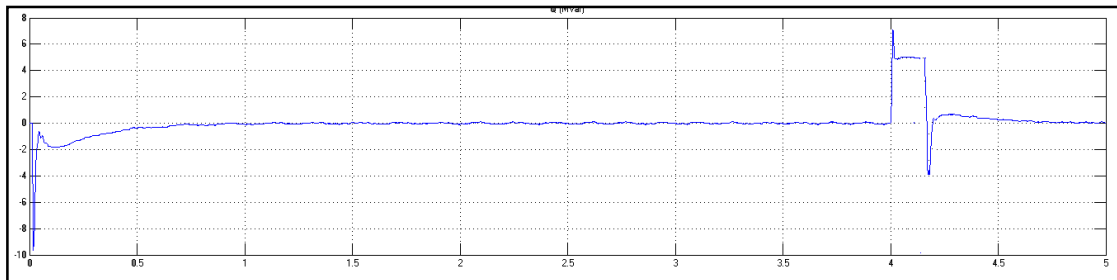


Fig. 7 (b) reactive power at off shore

IV. CONCLUSION

This paper has presented the performance analysis of the studied system containing DFIG OWF feeding into a power system through a hybrid HVDC system. Control schemes for the VSC and the LCC of the hybrid HVDC system has been presented. Through the time-domain simulation results, it is found that the dynamic responses of the studied system under the applied severe faults are stable. It can be seen from these results that the hybrid HVDC link can offer better performance to effectively mitigate the variations of OWFs under different wind speeds. The power transmitted through the DC line and the voltage across the DC line is maintained constant irrespective of the variations in wind speed.

REFERENCES

- [1]. A. Reidy and R. Watson, "Comparison of VSC based HVDC and HVAC interconnections to a large offshore wind farm," in Proc. IEEE Power Engineering Society General Meeting, vol. 1, pp. 1–8, June 2005
- [2]. L. Wang, K.-H. Wang, W.-J. Lee, and Z. Chen, "Power-Flow control and stability enhancement of four parallel-operated offshore wind farms using a line-commutated HVDC link," IEEE Trans. Power Delivery, vol. 25, no. 2, pp. 1190–1202, Apr. 2010.
- [3]. L. Guangkai, L. Gengyin, L. Haifeng, Y. Ming, and Z. Chengyong, "Operational mechanism and characteristic analysis of novel hybrid HVDC system," in Proc. IEEE Power System Technology, pp. 1–6, Oct. 2006.
- [4]. B. Qahraman, A. M. Gole, and I. T. Fernando, "Hybrid HVDC converters and their impact on power system dynamic performance," in Proc. IEEE Power Engineering Society General Meeting, pp. 18–22, Jun. 2006.
- [5]. B. R. Andersen and X. Lie, "Hybrid HVDC system for power transmission to island networks," IEEE Trans. Power Delivery, vol. 19, no. 4, pp. 1884–1890, Oct. 2004.
- [6]. L. Guangkai, L. Gengyin, L. Haifeng, Y. Ming, and Z. Chengyong, "Operational mechanism and characteristic analysis of novel hybrid HVDC system," in Proc. IEEE Power System Technology, pp. 1–6, Oct. 2006.
- [7]. B. R. Andersen and X. Lie, "Hybrid HVDC system for power transmission to island networks," IEEE Trans. Power Delivery, vol. 19, no. 4, pp. 1884–1890, Oct. 2004.
- [8]. R. E. Torres-Olguin, M. Molinas, and T. M. Undeland, "A model-based controller in rotating reference frame for Hybrid HVDC," in Proc. IEEE Energy Conversion Congress and Exposition, pp. 1578–1584, Sep. 2010.